J Mater Sci: Mater Electron (2017) 28:2415–2420
DOI 10.1007/s10854-016-5812-7

# Different morphologies fabrication of $NiAl_2O_4$ nanostructures with the aid of new template and its photocatalyst application

**Mehdi Rahimi-Nasrabadi[1,2] · Farhad Ahmadi[3,4] · Mohammad Eghbali-Arani[5]**

Received: 9 July 2016 / Accepted: 3 October 2016 / Published online: 8 October 2016


**Abstract** In the area of water purification, nanotechnology offers the possibility of an efficient removal of pollutants and germs. Nowadays, nanostructures used for detection and removal of chemical and biological substances include metals, azo dyes, nutrients, cyanide, organics, algae, bacteria, parasites, and etc. In the current study, an attempt is made to synthesize and characterization of $NiAl_2O_4$ nanostructures in an aqueous environment through the simple sol–gel method. Besides, three capping agents as glycine, asparagine, and alanine were used to investigate their effects on the morphology and particle size of $NiAl_2O_4$ nanostructures. This method starts from of the precursor complex, and involves the formation of homogeneous solid intermediates, reducing atomic diffusion processes during thermal treatment. The formation of pure crystallized $NiAl_2O_4$ nanocrystals occurred when the precursor was heat-treated at 800 °C in air for 150 min. The stages of the formation of $NiAl_2O_4$, as well as the characterization of the resulting compounds were done made using UV–Vis diffuse reflectance spectroscopy, field emission scanning electron microscopy, energy dispersive X-ray microanalysis, and X-ray diffraction. The magnetic properties of as-prepared $NiAl_2O_4$ nanostructures were also investigated with vibrating sample magnetometer. Furthermore, the photocatalytic properties of as synthesized $NiAl_2O_4$ were evaluated by degradation of methyl orange as water contaminant.

✉ Mehdi Rahimi-Nasrabadi
Rahiminasrabadi@gmail.com

✉ Farhad Ahmadi
Farhadahmadi55@gmail.com

[1] Faculty of Pharmacy, Baqiyatallah University of Medical Sciences, Tehran, Iran

[2] Department of Chemistry, Imam Hossein University, Tehran, Iran

[3] Physiology Research Center, Iran University of Medical Sciences, Tehran, Iran

[4] Department of Medicinal Chemistry, School of Pharmacy-International Campus, Iran University of Medical Sciences, Tehran, Iran

[5] Department of Physics, University of Kashan, Kashan, Iran

## 1 Introduction

Physical properties and potential applications of nanostructures and nanomaterial have been studied intensively [1–12]. This interest results from the special properties of materials at the nanoscale, such as a large surface-to-volume ratio and increased surface activity, as compared with that of the bulk material. The properties of bulk materials usually depend on the size of the primary particles. Thus, the control of particle size and morphology plays a crucial role in the manufacturing process [13–15]. Transition metal-oxide spinels are important in many application fields because of their high thermal resistance and catalytic, electronic and optical properties. They are commonly used in semiconductor and sensor technology as well as in heterogeneous catalysis [16–24]. Transition metal aluminates are commonly prepared by a solid state reaction [25], co-precipitation method [26], hydrothermal [27], combustion [28], and sol–gel [29, 30]. The disadvantages of solid-state routes, such as inhomogeneity, lack of stoichiometry control, high temperature and low surface area, are improved when the material is synthesized using a solution-based method. Compared with other techniques, the sol–gel method is a useful and attractive technique for the preparation of aluminate spinels because of its advantage

**Table 1** Preparation conditions for the synthesis of $NiAl_2O_4$ nanostructures

| Sample no. | Capping agent | Temperature (°C) | Decolorization (%) |
|---|---|---|---|
| 1 | Glycine | 800 | 82 |
| 2 | Asparagine | 800 | – |
| 3 | Alanine | 800 | – |

of producing pure and ultrafine powders at low temperatures. In this study, we have synthesized nickel aluminate nanocrystals using simple sol–gel method. Furthermore, to investigate the effect of different capping agents such as glycine, asparagine, and alanine on the morphology, particle size, and crystal structure of the products several experiments were performed. To evaluate the catalytic properties of nanocrystalline nickel aluminate, the photocatalytic degradation of methyl orange under UV light irradiation was carried out.

## 2 Experimental

### 2.1 Characterization

All the chemicals used in this method were purchased from Merck Company and used without further purification. X-ray diffraction (XRD) patterns were recorded by a Philips-X'PertPro, X-ray diffractometer using Ni-filtered Cu K$\alpha$ radiation at scan range of $10 < 2\theta < 80$. Scanning electron microscopy (SEM) images were obtained on LEO-1455VP equipped with an energy dispersive X-ray spectroscopy. Spectroscopy analysis (UV–Vis) was carried out using Shimadzu UV–Vis scanning UV–Vis diffuse reflectance spectrometer. The energy dispersive spectrometry (EDS) analysis was studied by XL30, Philips microscope. The magnetic measurements of samples were carried out in a vibrating sample magnetometer (VSM) (Meghnatis Daghigh Kavir Co.; Kashan Kavir; Iran) at room temperature in an applied magnetic field sweeping between ±10,000 Oe.

### 2.2 Synthesis of $NiAl_2O_4$ nanostructures

At first, 1 mmol of $Ni(NO_3)_2{\cdot}6H_2O$ and 2 mmol of $Al(NO_3)_3{\cdot}9H_2O$ were dissolved separately in 40 ml distilled water and stirred for 10 min. Then, a solution containing 1 mmol of amino acid was added drop wise into a solution involving 1 mmol of $Ni(NO_3)_2{\cdot}6H_2O$. Subsequently, above mention solution was mixed with solution containing 2 mmol of $Al(NO_3)_3{\cdot}9H_2O$. Afterwards, the final mixed solution was kept stirring to form a gel at 100 °C. Finally, the obtained product was placed in a conventional furnace in air atmosphere for 150 min and calcine at 800 °C. After thermal treatment, the system was allowed to cool to room temperature naturally, and the obtained precipitate was collected. Reaction conditions are listed in Table 1.

### 2.3 Photocatalysis experiments

The photocatalytic activities of $NiAl_2O_4$ nanocrystal were determined by the degradation of aqueous methyl orange (MO) under UV light. About 0.1 g of the sample was first inserted into a reactor that included 50 ppm of aqueous MO. The suspension was transferred into a self-designed glass reactor, and stirred in darkness to attain the adsorption equilibrium. In the research of photo degradation by UV light, a 400 W mercury lamp with a water cooling cylindrical jacket was utilized. The photocatalytic activity of $NiAl_2O_4$ nanostructure was tested by using methyl orange (MO) solution. The degradation reaction was carried out in a quartz photocatalytic reactor. The photocatalytic degradation was carried out with 50 ppm of MO solution containing 0.1 g of nanostructures. This mixture was aerated for 30 min to reach adsorption equilibrium. Then, the mixture was placed inside the photoreactor in which the vessel was 20 cm away from the UV. The quartz vessel and light sources were placed inside a black box equipped with a fan to prevent UV leakage. Aliquots of the mixture were taken at periodic intervals during the irradiation, and after centrifugation they were analyzed with the UV–Vis spectrometer. The methyl orange (MO) degradation percentage was calculated as:

$$\text{Degradation rate } (\%) = 100(A_0 - A_t)/A_0 \quad (1)$$

where $A_t$ and $A_0$ are the obtained absorbance value of the methyl orange solution at t and 0 min by a UV–Vis spectrometer, respectively.

## 3 Results and discussion

Crystalline structure and phase purity of as-prepared product has been determined using XRD. The XRD pattern of as-prepared $NiAl_2O_4$ is shown in Fig. 1. Based on the Fig. 1, the diffraction peaks observed can be indexed to the pure tetragonal phase of $NiAl_2O_4$ ($a = b = 5.9366$ Å, $c = 14.5430$ Å) with space group of R-3 m and JCPDS no. 01-1299. No diffraction peaks from other species could be detected, which indicates the obtained sample is pure.

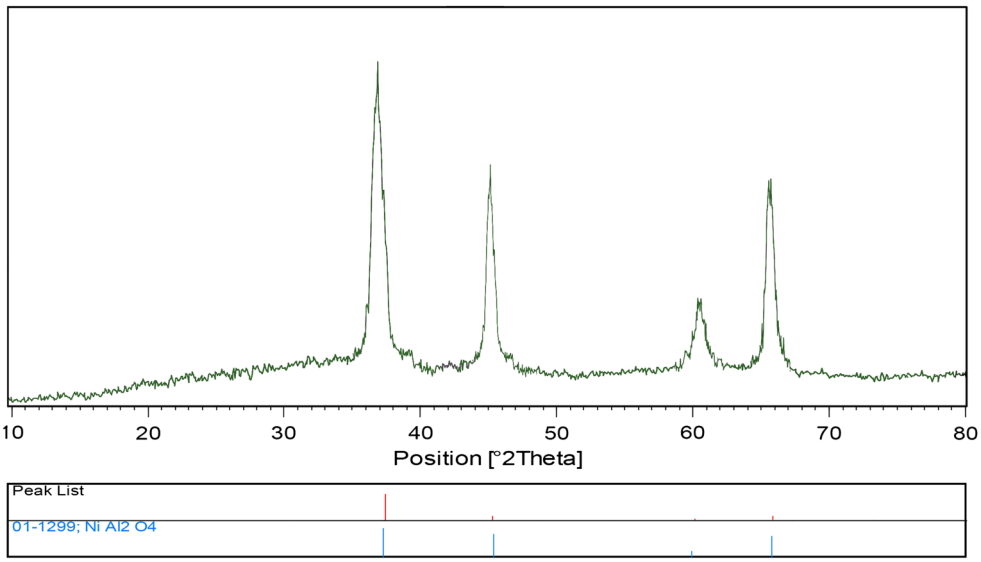


**Fig. 1** XRD patterns of the sample no. 1 after calcinacion at 800 °C

From XRD data, the crystallite diameter ($D_c$) of $NiAl_2O_4$ nanostructures was calculated to be 13 nm using the Scherer equation:

$$D_c = K\lambda/\beta\cos\theta \qquad \text{Scherer equation}$$

where $\beta$ is the breadth of the observed diffraction line at its half intensity maximum (400), K is the so-called shape factor, which usually takes a value of about 0.9, and $\lambda$ is the wavelength of X-ray source used in XRD. Capping agents and surfactants are frequently used in colloidal synthesis to inhibit nanostructures overgrowth and aggregation as well as to control the structural characteristics of the resulted nanostructures in a precise manner [31–41]. In this research glycine, asparagine, and alanine used as capping agent to investigate their effect on the morphology and particle size of the $NiAl_2O_4$ nanostructures. Figure 2a–c shows the SEM images of $NiAl_2O_4$ nanostructures in the presence glycine, asparagine, and alanine as the capping agent accordance with sample 1–3, respectively. According to the Fig. 2a, product mainly consists of spherical shape nanostructures with average particle size 35–40 nm. Furthermore in the presence of alanine the products mainly consist of nanorod, as shown in Fig. 2c. The EDS analysis measurement was used to investigate the chemical composition and purity of $NiAl_2O_4$ nanostructures. According to the Fig. 3, the product consists of Ni, Al, and O elements. Furthermore, neither N nor C signals were detected in the EDS spectrum, which means the product is pure and free of any surfactant or impurity. The VSM magnetic measurements for the nickel aluminate oxide (Fig. 4) show the magnetic properties of nanostructures calcined at 800 °C. The $NiAl_2O_4$ nanostructure (sample 1) exhibits paramagnetic behavior at room temperature with a magnetization of 0.12 emu/g. To investigate the optical properties of the $NiAl_2O_4$, UV–Vis spectrum was recorded. Figure 5 shows the UV–Vis diffuse reflectance spectrum of $NiAl_2O_4$ nanostructures. Using Tauc's formula, the band gap can be obtained from the absorption data. The energy gap (Eg) of the nanocrystalline $NiAl_2O_4$ has been estimated by extrapolating the linear portion of the plot of $(\alpha h\nu)^2$ against $h\nu$ to the energy axis. The Eg value of the nanocrystalline $NiAl_2O_4$ calculated to be 3.1 eV. According to the obtained Eg value, as-prepared nanostructures $NiAl_2O_4$ sample can be employed as the photocatalyst. Photodegradation of methyl orange as water contaminant under UV light illumination was employed to evaluate the properties of the as-synthesized $NiAl_2O_4$ nanostructures. Figure 6 exhibits the obtained result. No methyl orange was practically broken down after 80 min without employing UV light illumination or as-prepared $NiAl_2O_4$ nanostructures. This observation illustrated that the contribution of self-degradation was insignificant. The proposed mechanism of the photocatalytic degradation of the methyl orange can be assumed as:

$$NiAl_2O_4 + h\nu \rightarrow NiAl_2O_4^{\cdot} + e^- + h^+ \qquad (2)$$

$$h^+ + H_2O \rightarrow OH^{\cdot} \qquad (3)$$

$$e^- + O_2 \rightarrow O_2^{\cdot -} \qquad (4)$$

$$OH^{\cdot} + O_2^{\cdot -} + \text{methyl orange} \rightarrow \text{Degradation products} \qquad (5)$$

Utilizing photocatalytic calculations by Eq. (1), the methyl orange degradation was about 82 % after 80 min illumination of UV light in the presence of $NiAl_2O_4$ nanostructures (sample 1). Besides, the whole mechanism is shown in Scheme 1.

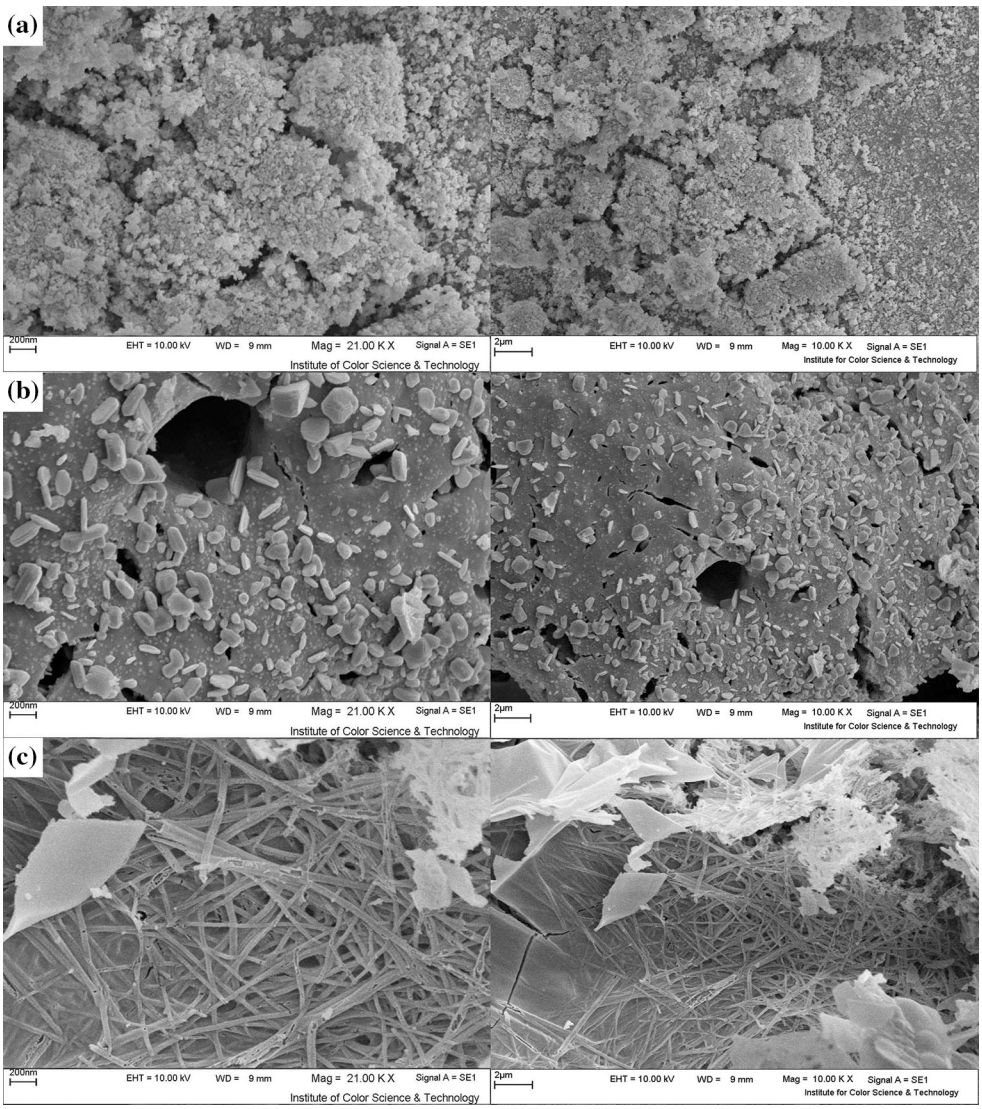


**Fig. 2** SEM images of $NiAl_2O_4$ nanostructures calcinacion at 800 °C. **a** Sample 1, **b** sample 2 and **c** sample 3

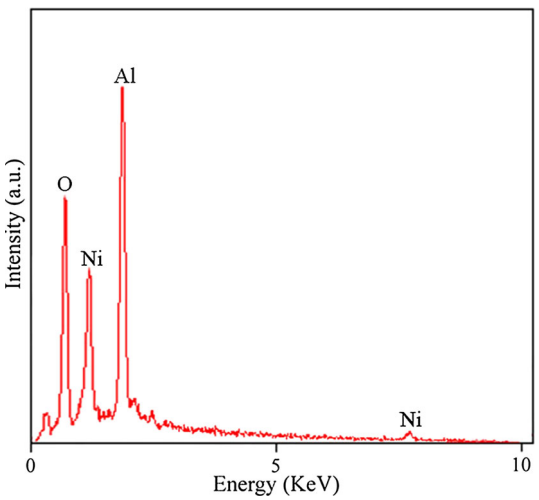


**Fig. 3** EDS pattern of $NiAl_2O_4$ nanostructures synthesized at 800 °C

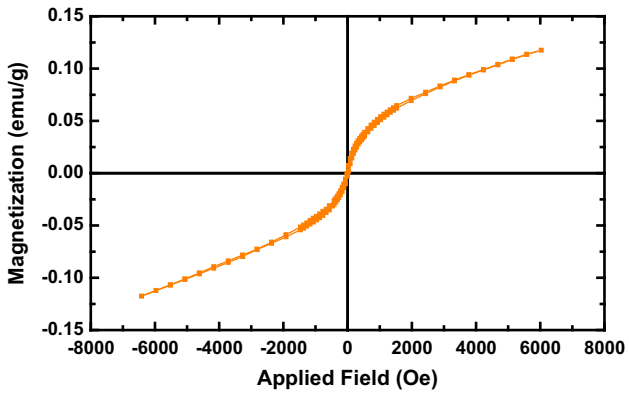


**Fig. 4** VSM curves of $NiAl_2O_4$ nanostructures calcinacion at 800 °C

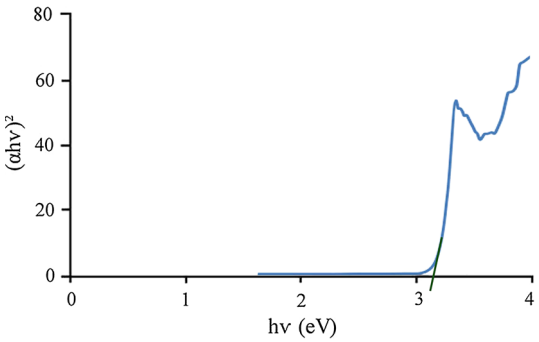


**Fig. 5** DRS pattern of $NiAl_2O_4$ nanostructures synthesized at 800 °C

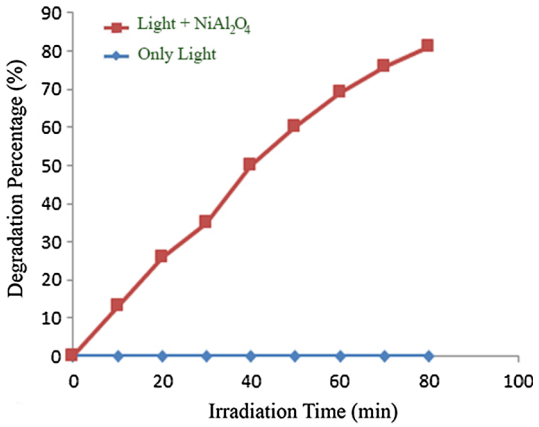


**Fig. 6** Photocatalytic methyl orange degradation of $NiAl_2O_4$ nanostructures (sample 1) under ultraviolet light

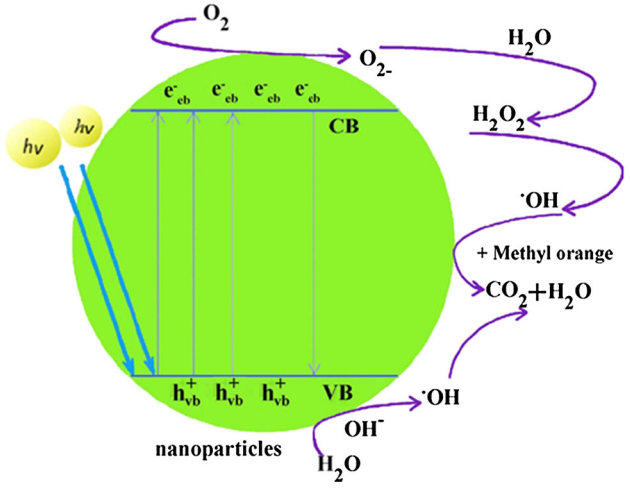


**Scheme 1** Reaction mechanism of methyl orange photodegradation over $NiAl_2O_4$ nanostructures under UV light irradiation

## 4 Conclusions

A facile method is described for synthesizing nanorod and spherical shape nanostructures via a simple sol–gel method in the presence of glycine, asparagine, and alanine as the natural capping agents. Besides, several tests were performed to investigate the effects of natural capping agents on them morphology and particle size of final products. The nickel aluminate oxide nanoparticles exhibit superparamagnetic behaviour at room temperature, with saturation magnetization of 0.12 emu/g. Furthermore, in order to evaluate the photocatalytic properties of nanocrystalline $NiAl_2O_4$, the photocatalytic degradations of simulated methyl orange dye wastewater under ultraviolet light irradiation were carried out.

**Acknowledgments** The authors are grateful to council of University of Kashan for providing financial support to undertake this work by Grant No (572801/2).

## References

1. V. Arabali, M. Ebrahimi, M. Abbasghorbani, V. KumarGupta, M. Farsi, M.R. Ganjali, F. Karimi, J. Mol. Liq. **213**, 312 (2016)
2. H.R. Naderi, P. Norouzi, M.R. Ganjali, Appl. Surf. Sci. **366**, 552 (2016)
3. S.M. Hosseinpour-Mashkani, A. Sobhani-Nasab, J. Mater. Sci.: Mater. Electron. **27**, 3240 (2016)
4. M. Zahraei, A. Monshi, D. Shahbazi-Gahrouei, M. Amirnasr, B. Behdadfar, M. Rostami, J. Nanostruct. **5**, 137 (2015)
5. M. Rahimi-Nasrabadi, J. Nanostruct. **4**, 211 (2014)
6. M. Maddahfar, M. Ramezani, M. Sadeghi, A. Sobhani-Nasab, J. Mater. Sci.: Mater. Electron. **26**, 7745 (2015)
7. S. Khaleghi, J. Nanostruct. **2**, 157 (2012)
8. M. Aliahmad, A. Rahdar, Y. Azizi, J. Nanostruct. **4**, 145 (2014)
9. M. Enhessari, M. Kargar-Razi, P. Moarefi, A. Parviz, J. Nanostruct. **2**, 119 (2012)
10. M. Behpour, M. Mehrzad, S.M. Hosseinpour-Mashkani, J. Nanostruct. **5**, 183 (2015)
11. M. Riazian, J. Nanostruct. **4**, 433 (2014)
12. M. Rahimi-Nasrabadi, M. Behpour, A. Sobhani-Nasab, S.M. Hosseinpour-Mashkani, J. Mater. Sci.: Mater. Electron. **26**, 9776 (2015)
13. S.M. Hosseinpour-Mashkani, M. Maddahfar, A. Sobhani-Nasab, J. Mater. Sci.: Mater. Electron. **27**, 474 (2016)
14. S.S. Hosseinpour-Mashkani, S.S. Hosseinpour-Mashkani, A. Sobhani-Nasab, J. Mater. Sci.: Mater. Electron. **27**, 4351 (2016)
15. K. Saberyan, N.S. Mazhari, M. Rahiminezhad-Soltani, M.A. Mohsen, J. Nanostruct. **4**, 185 (2014)
16. C.O. Areán, M.P. Mentruit, E.E. Platero, F.X. Xamena, J.B. Parra, Mater. Lett. **39**, 22 (1999)
17. E.E. Platero, C.O. Areán, J.B. Parra, Res. Chem. Intermed. **25**, 187 (1999)
18. J. Merikhi, H.O. Jungk, C. Feldmann, J. Mater. Chem. **10**, 1311 (2000)
19. W. Li, J. Li, J. Guo, J. Eur. Ceram. Soc. **23**, 2289 (2003)
20. D.M.A. Melo, J.D. Cunha, J.D.G. Fernandes, M.I. Bernardi, M.A.F. Melo, A.E. Martinelli, Mater. Res. Bull. **38**, 1559 (2003)
21. P. Thorma-hlen, E. Fridell, N. Cruise, M. Skoglundh, A. Palmqvist, Appl. Catal. B Environ. **31**, 1 (2001)
22. W.M. Shaheen, Thermochim. Acta **385**, 105 (2002)
23. G.A.E. Shobaky, G.A. Fagal, N.H. Amin, Thermochim. Acta **141**, 205 (1989)
24. L. Dussault, J.C. Dupin, C. Guimon, M. Monthioux, N. Latorre, T. Ubieto, E. Romeo, C. Royo, A. Monzon, J. Catal. **251**, 223 (2007)

25. W.S. Hong, L.C. De-Jonghe, X. Yang, M.N. Rahaman, J. Am. Ceram. Soc. **78**, 3217 (1995)
26. T. Mimani, J Alloy Comp **315**, 123 (2001)
27. M. Zawadzki, J. Wrzyszcz, Mater. Res. Bull. **35**, 109 (2000)
28. A.K. Adak, A. Pathak, P. Pramanik, J. Mater. Sci. Lett. **17**, 559 (1998)
29. M. Zayat, D. Levy, Chem. Mater. **12**, 2763 (2000)
30. N. Guilhaume, M. Primet, J. Chem. Soc. Faraday Trans. **90**, 1541 (1994)
31. J. Safaei-Ghomi, S. Zahedi, M. Javid, M.A. Ghasemzadeh, J. Nanostruct. **5**, 153 (2015)
32. M. Rahimi-Nasrabadi, S.M. Pourmortazavi, A.A. Davoudi-Dehaghani, S.S. Hajimirsadeghi, M.M. Zahedi, Cryst. Eng. Comm. **15**, 4077 (2013)
33. M. Behpour, M. Chakeri, J. Nanostruct. **2**, 227 (2012)
34. S.M. Pourmortazavi, M. Taghdiri, V. Makari, M. Rahimi-Nasrabadi, Spectrochim. Acta A Mol. Biomol. Spectrosc. **136**, 1249 (2015)
35. M. Rahimi-Nasrabadi, S.M. Pourmortazavi, M.R. Ganjali, Mater. Manuf. Process. **30**, 34 (2015)
36. S.M. Pourmortazavi, M. Rahimi-Nasrabadi, S.S. Hajimirsadeghi, J. Dispers. Sci. Technol. **33**, 254 (2012)
37. S.M. Hosseinpour-Mashkani, M. Ramezani, A. Sobhani-Nasab, M. Esmaeili-Zare, J. Mater. Sci. Mater. Electron. **26**, 6086 (2015)
38. A. Sobhani-Nasab, M. Maddahfar, S.M. Hosseinpour-Mashkani, J. Mol. Liq. **216**, 1 (2016)
39. S.M. Pourmortazavi, M. Rahimi-Nasrabadi, M. Khalilian-Shalamzari, H.R. Ghaeni, S.S. Hajimirsadeghi, J. Inorg. Organomet. Polym Mater. **24**, 333 (2014)
40. M. Rahimi-Nasrabadi, S.M. Pourmortazavi, M.R. Ganjali, S.S. Hajimirsadeghi, M.M. Zahedi, J. Mol. Struct. **1047**, 31 (2013)
41. S.M. Pourmortazavi, M. Rahimi-Nasrabadi, A.A. Davoudi-Dehaghani, A. Javidan, M.M. Zahedi, S.S. Hajimirsadeghi, Mater. Res. Bull. **47**, 1045 (2012)